

Deafening-induced rapid changes to spine synaptic connectivity in the adult avian vocal basal ganglia

Xiaojuan ZHOU,^{1,2} Yalan CHEN,^{1,3} Jikan PENG,^{1,4} Mingxue ZUO¹ and Yingyu SUN¹

¹Beijing Key Laboratory of Gene Resource and Molecular Development, College of Life Sciences, Beijing Normal University, Beijing, China, ²Chinese Institute for Brain Research (CIBR), Beijing, China, ³Technology Center for Protein Sciences, Tsinghua University, Beijing, China and ⁴School of Life Sciences, Westlake University, Hangzhou, China

Abstract

The basal ganglia have been implicated in auditory-dependent vocal learning and plasticity in human and songbirds, but the underlying neural phenotype remains to be clarified. Here, using confocal imaging and three-dimensional electron microscopy, we investigated striatal structural plasticity in response to hearing loss in Area X, the avian vocal basal ganglia, in adult male zebra finch (*Taeniopygia guttata*). We observed a rapid elongation of dendritic spines, by approximately 13%, by day 3 after deafening, and a considerable increase in spine synapse density, by approximately 61%, by day 14 after deafening, compared with the controls with an intact cochlea. These findings reveal structural sensitivity of Area X to auditory deprivation and suggest that this striatal plasticity might contribute to deafening-induced changes to learned vocal behavior.

Key words: basal ganglia, dendritic spine, songbird, synapse, vocal plasticity

INTRODUCTION

Learned vocalization, such as birdsong and human speech, is a unique motor skill that relies on auditory feedback (Doupe *et al.* 2005; Jarvis 2019). Its underlying neural substrates remain to be clarified. The basal ganglia have been strongly implicated in motor functions, including vocal learning and plasticity (Graybiel *et al.* 1994; Graybiel 2005; Bolhuis *et al.* 2010; Fee & Goldberg 2011; Simonyan *et al.* 2012; Raghanti *et al.* 2016; Jarvis 2019). Songbirds, such as zebra finch (*Taeniopygia guttata*), possess a discrete basal ganglia nucleus, known as Area X,

which is specifically dedicated to song behavior (Doupe *et al.* 2005; Gale & Perkel 2010). Understanding the processes within avian Area X might help elucidate the exact role of the basal ganglia circuit in learned vocalizations (Doupe *et al.* 2005) and may inform human speech processing (Pfenning *et al.* 2014; Simmonds *et al.* 2014).

Area X, together with 2 downstream nuclei, the anterior portion of the dorsal lateral nucleus of the medial thalamus (aDLM, Horita *et al.* 2012) and the lateral part of the magnocellular nucleus of the nidopallium (LMAN), forms the anterior forebrain pathway (AFP), which is homologous to the basal ganglia-thalamo-cortical circuit in mammals (Doupe *et al.* 2005). Accumulating evidence indicates the essential role of the AFP in adult song plasticity. For example, while stereotyped songs of adult zebra finch degrade following deafness (Nordeen & Nordeen 1992; Lombardino & Nottebohm 2000; Horita *et al.* 2008;

Correspondence: Yingyu Sun, College of Life Sciences, Beijing Normal University, No 19. Xijiekouwai Street, Haidian District, Beijing 100875, China.
Email: sunyingyu@bnu.edu.cn

Tschida & Mooney 2012), these vocal changes can be prevented by lesioning either the LMAN, the output nucleus of the AFP (Brainard & Doupe 2000; Horita *et al.* 2008), or Area X, the input (Kojima *et al.* 2013), before deafening. Further, we have previously reported that deafening-induced vocal changes and dendritic spine remodeling in the robust nucleus of the arcopallium (RA, the vocal motor nucleus), a motor cortex analog, both depend on an intact Area X (Zhou *et al.* 2017). Hence, Area X likely provides neural substrates to drive this cortical plasticity and subsequent behavioral changes.

Area X contains typical neurons found in both the mammalian striatum and globus pallidus (Farries & Perkel 2002; Farries *et al.* 2005; Goldberg & Fee 2010; Goldberg *et al.* 2010), the main input and output nuclei of the mammalian basal ganglia, respectively (Fazl & Fleisher 2018). The vast majority of Area X neurons are striatal spiny neurons with moderately to densely spiny dendrites, while the remaining striatal interneurons and pallidal neurons are characterized by smooth dendrites (Farries & Perkel 2002; Gale & Perkel 2010). Similar to their counterparts in mammals, the spiny neurons receive robust excitatory glutamatergic afferents from the pallium and dense dopaminergic innervation from the midbrain (Ding & Perkel 2002; Farries *et al.* 2005). They thus integrate large extrinsic inputs to influence the basal ganglia activity by sending the output to pallidal neurons (Farries *et al.* 2005; Kreitzer & Malenka 2008) and may represent a major site of synaptic plasticity in the basal ganglia (Ding & Perkel 2002; Kreitzer & Malenka 2008; Thompson & Perkel 2011).

Dendritic spines are the main postsynaptic targets of excitatory glutamatergic inputs and remarkably plastic structures for long-term changes in synaptic connections (Chen *et al.* 2014; Villalba & Smith 2018; Chidambaram *et al.* 2019). Numerous studies in mammals indicate a close link between striatal plasticity and procedural learning (Perrin & Venance 2019), as well as brain disorders (Villalba & Smith 2018). For example, changes in the number of spines (McNeill *et al.* 1988; Ingham *et al.* 1989) and the morphology of glutamatergic axospinous synapses (Villalba *et al.* 2015) in the striatum have been documented in both, individuals with Parkinson's disease, and animal models of this disease. In particular, selective strengthening of specific corticostriatal synapses was observed during the acquisition of an auditory discrimination task (Xiong *et al.* 2015). We therefore hypothesized that striatal synaptic modifications also occur over the course of auditory feedback-related vocal plasticity. Here, we report rapid changes in spine morphology and spine synapse numbers in Area X that accompany deafening-

induced song degeneration in adult zebra finch. Our findings provide structural insights into striatal plasticity in response to hearing loss that improve the understanding of the contributions of the basal ganglia to vocal motor plasticity.

MATERIALS AND METHODS

Animals and surgery

Thirty-one adult male zebra finches (4–6 month old) were used in the current study, with 25 used in DiI labeling and confocal microscopy experiments, and 6 used in three-dimensional (3D) electron microscopy experiments. The zebra finches were purchased from a local supplier and housed at the authors' laboratory, under a 12:12 h light/dark cycle, with food and water available *ad libitum*. Birds were deafened by a bilateral removal of the cochlea, as described by Li *et al.* (2013), and were analyzed on days 3 or 14 after deafening. The protocol was approved by the Animal Management Committee of the College of Life Sciences, Beijing Normal University.

Song analysis

Birds were housed individually in sound-attenuated chambers for song recording with the aid of Sound Analysis Pro software (version 2011.104, Tchernichovski *et al.* 2000). Two syllable spectral features, that is, Wiener entropy and entropy variance, were measured using the same software to evaluate the effects of deafening on song structure, as described previously (Horita *et al.* 2008; Tschida & Mooney 2012; Zhou *et al.* 2017). Syllables within the first dominant motif from 30 song bouts were selected for analysis for each bird at each time point. For each measure, a baseline was set for each syllable, by averaging the values from 2 days pre-deafening (0–14 days before deafening). The change in each measure for each syllable on the last survival day was calculated as a percentage of the baseline. A single value for each bird was obtained by averaging the ratios of all syllables within each bird.

DiI labeling and confocal microscopy

Area X spiny neurons and their dendrites of 25 birds were fluorescently labeled using the carbocyanine dye DiI (D-282, Molecular Probes), as described elsewhere (Zhou *et al.* 2017). Briefly, the birds were intracardially perfused with 1.5% paraformaldehyde (PFA) in 0.1 M phosphate buffer (PB) following a lethal dose of urethane. The brain

was then dissected and sliced along the coronal plane into 100- μm sections using a vibratome. Sonicated DiI fine powder was then carefully scattered over Area X under a dissecting microscope using a glass micropipette with a sharp tip. The sections were overlaid with PB and incubated at room temperature for 12 h in the dark, allowing the dye to diffuse along the dendritic membranes. Finally, the sections were fixed with 4% PFA for 30 min, rinsed with PB, and mounted with antifade mounting medium, and imaged.

The sections were imaged using a Zeiss LSM 700 confocal microscope. Laser light at a 555-nm wavelength was used to excite DiI. For each bird, at least 6 Area X neurons were randomly sampled. For each neuron, 2 to 4 second- or third-order dendritic segments (25–60 μm) were imaged under a 40 \times oil-immersion objective (NA 1.3), at a 1024 \times 1024 pixel resolution, with a z-step of 0.2 μm . Image stacks were then deconvoluted using AutoQuant software (Media Cybernetics). Dendritic spines were analyzed blindly as described by Zhou *et al.* (2017), using NeuronStudio software (Rodríguez *et al.* 2008).

3D electron microscopy

Six birds were intracardially perfused with 0.9% NaCl under an overdose of urethane. The birds were then perfused with 2.5% glutaraldehyde and 2% PFA in 0.1 M PB. The brain was dissected and sliced along the sagittal plane into 100- μm sections using a vibratome. A piece of Area X tissue was punched under a dissecting microscope and sequentially post-fixed with 1% osmium tetroxide and 1.5% potassium ferrocyanide in double-distilled water (ddH₂O), 1% thiocarbohydrazide in ddH₂O, and 1% osmium tetroxide in ddH₂O. After *en bloc* staining with 2% uranyl acetate, the fixed tissue pieces were dehydrated in a graded series of alcohol solutions and then flat-embedded in SPI-Pon 812 medium.

3D-Images of the Area X neuropil were acquired using a combined focused ion beam/scanning electron microscope (FIB/SEM, Helios Nanolab 600i, FEI). Image stacks were obtained automatically by sequential FIB milling and SEM imaging at a 2048 \times 1768 pixel resolution (x, y: 4.9 nm/pixel), with a z-step (section thickness) of 30 nm, avoiding cell somata and the blood vessels to the greatest extent possible. Each image stack served as a 3D sample of the tissue. For each sample, a volume of between 237.08 and 612.11 μm^3 (mean, 418.64 μm^3) was examined. Synapses within these volumes were visualized and automatically segmented in 3D using Espina Interactive Neuron Analyzer (EspINA) software (version

2.8.2, Morales *et al.* 2011). The synapses were identified based on the observation of a postsynaptic density (PSD) and presynaptic vesicles adjacent to PSD (Merchán-Pérez *et al.* 2009). Synapses located on dendritic spines were observed by navigating the stack of serial sections.

Synapses within an unbiased 3D counting frame were directly counted using EspINA. The synapse density was determined by dividing the total number of synapses counted by the volume of the frame. The size of each synapse was evaluated by measuring the area and perimeter of the synaptic apposition surface (SAS). The SAS, extracted from the 3D segmented synapse using EspINA, represents the surface of apposition between the pre- and postsynaptic density, and provides the morphological features of the synapse (Morales *et al.* 2013). The analyses were performed by an investigator blinded to the experimental conditions.

Statistical analysis

All data were analyzed using GraphPad Prism 7 for Windows (GraphPad Software, Inc.). One-sample Kolmogorov–Smirnov test (KS) was used to assess normality. One-way analysis of variance (ANOVA), followed by Tukey's multiple comparison test, was used to compare the spine density and morphology data among the 3 experimental groups (control, deaf 3d, and deaf 14d). Unpaired *t*-test was used to compare the numbers and types of spine synapses between the control and deaf 14d groups. Two-sample KS test was used to compare cumulative frequency distributions for spine morphology and SAS data. Nonparametric Kruskal–Wallis test (KW), followed by Dunn's multiple comparison test, was used to compare the changes in syllable features among the 3 experimental groups. Two-tailed *P*-values < 0.05 were considered statistically significant. Graphs were plotted using GraphPad Prism 7. All data are presented as the mean \pm SEM. No data presented in the current study have been previously published.

RESULTS

We first examined the effect of hearing loss on spine density and morphology. The dendrites and dendritic spines of Area X spiny neurons were stained well with the fluorescent dye DiI (Fig. 1a). We analyzed 4380 spines on 218 dendritic segments of 93 cells in 9 control birds with an intact cochlea; 4616 spines on 223 dendritic segments of 87 cells in 8 deafened birds 3 days after deafening (deaf 3d); 4908 spines on 225 dendrites of 96 cells in 8 deafened birds 14 days after deafening (deaf 14d). The

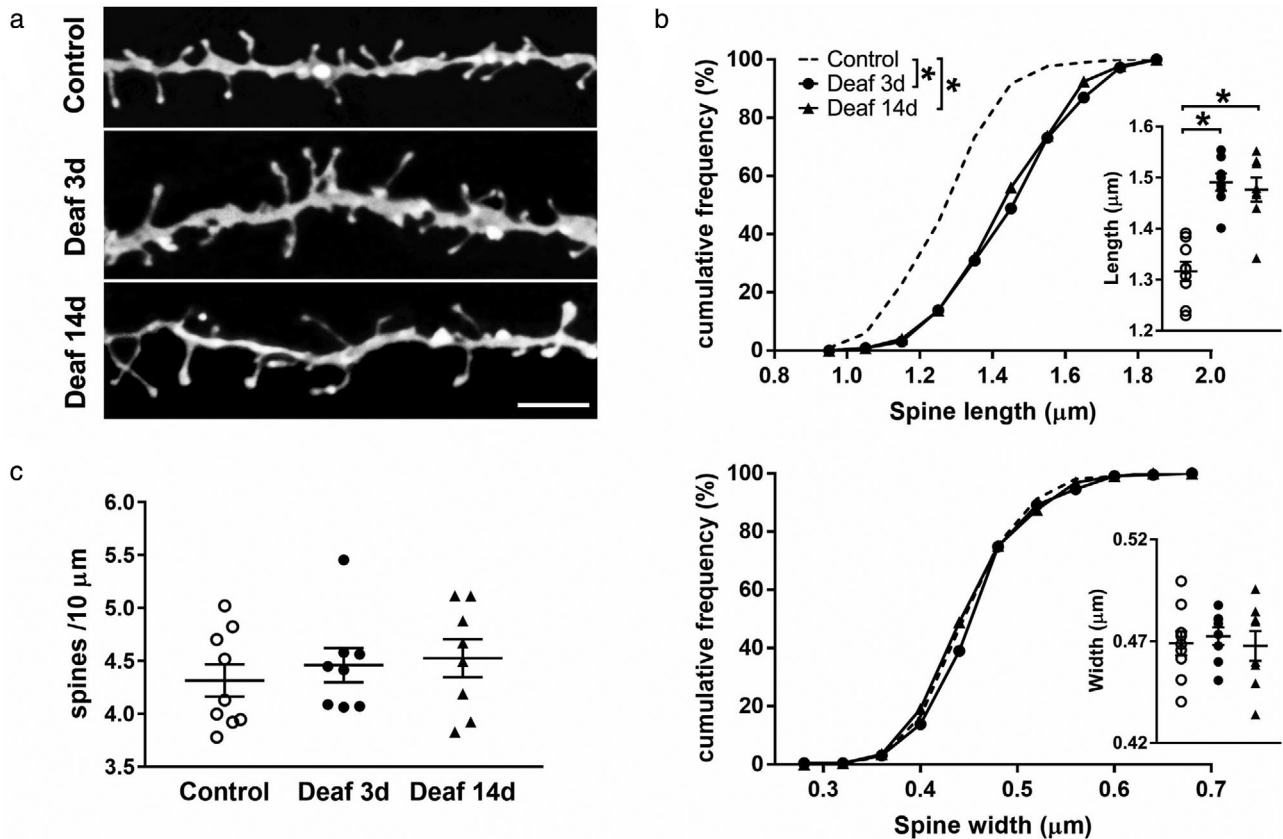


Figure 1 Effects of deafening on dendritic spines in adult Area X. (a) Representative images of dendritic segments of spiny neurons in Area X from a control bird, and 2 deafened birds on days 3 (deaf 3d) and 14 (deaf 14d) following deafness. Scale bars, 5 μm . (b) Major plots: Cumulative frequency distributions of the spine length (top) and width (bottom) averaged per dendrite in the 3 groups. $*P < 0.0001$, deaf 3d versus deaf 14d: $P > 0.05$, KS. Insets: Dot-plots show the mean values for each bird in each group (with mean \pm SEM overlapped, one point per bird; top, inset: length, control: $1.32 \pm 0.02 \mu\text{m}$, deaf 3d: $1.49 \pm 0.02 \mu\text{m}$, deaf 14d: $1.48 \pm 0.02 \mu\text{m}$, $F_{2,22} = 24.44$, $P < 0.0001$, ANOVA; bottom, inset: width, control: $0.47 \pm 0.006 \mu\text{m}$, deaf 3d: $0.47 \pm 0.004 \mu\text{m}$, deaf 14d: $0.47 \pm 0.007 \mu\text{m}$, $F_{2,22} = 0.163$, $P > 0.05$, ANOVA). $*P < 0.0001$, deaf 3d versus deaf 14 d: $P > 0.05$, ANOVA and Tukey's multiple comparison test. (c) Dot-plots of the mean spine density value for each bird in the 3 groups (with mean \pm SEM superimposed, one point per bird; control: 4.32 ± 0.15 spines/10 μm , deaf 3d: 4.46 ± 0.16 spines/10 μm , deaf 14d: 4.53 ± 0.18 spines/10 μm , $F_{2,22} = 0.445$, $P > 0.05$, ANOVA). The mean values for each bird were obtained from analyzing spines on 2 to 4 second- or third-order dendritic segments from at least 6 neurons.

spine length was increased rapidly by approximately 13% by day 3 after deafening and was then maintained without a further significant change until day 14 after deafening (Fig. 1b, top panel), whereas the spine width (Fig. 1b, bottom panel) and spine density (Fig. 1c) did not show measurable changes following deafness compared with the controls at any time point examined.

We then evaluated deafening-induced vocal changes in the same set of birds. Two acoustic features, Wiener entropy and entropy variance, are reported to be the parameters most sensitive to deafness (Horita *et al.* 2008; Tschida & Mooney 2012). Changes in these parameters

after deafening require an intact AFP (Horita *et al.* 2008; Zhou *et al.* 2017). We observed remarkable changes in syllables in terms of both mean entropy and entropy variance 14 days after deafening but not 3 days after deafening, compared with the controls (Fig. 2a,b; Fig. S1, Supporting Information). Although others have reported some changes in these 2 parameters already within a few days of deafening (Horita *et al.* 2008; Tschida & Mooney 2012), the changes occurred gradually during the first 2 weeks following deafness (Horita *et al.* 2008). In the current study, the spines in adult Area X were elongated to a similar extent on days 3 and 14 after

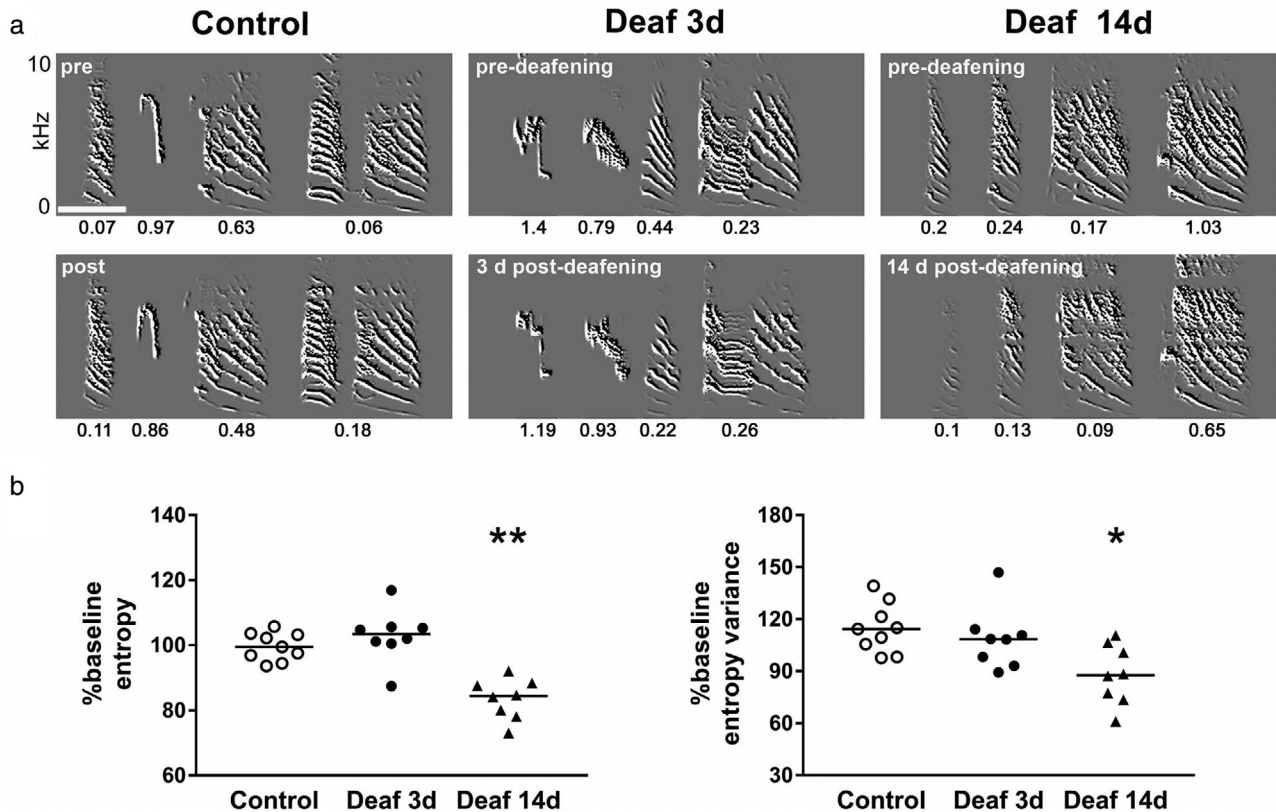


Figure 2 Spectral structure degradation of song following deafness. (a) Examples of pre- and post-deafening song spectrograms. The mean entropy variance value is shown below each syllable. Scale bar, 100 ms. (b) Dot-plots of deafening-induced changes in the syllable mean entropy and entropy variance. Changes to the syllables, presented as percentage of baseline, were averaged for each bird in the 3 groups (control: $n = 9$ birds, deaf 3d: $n = 8$ birds, deaf 14d: $n = 8$ birds; entropy, control versus deaf 3d: $P > 1.0$, control versus deaf 14d: $**P = 0.0076$; entropy variance, control versus deaf 3d: $P > 1.0$, control versus deaf 14d: $*P = 0.0128$; KW and Dunn's multiple comparison tests). The horizontal line in each plot denotes the median.

deafening compared with the spine length in the controls. Taken together, the presented findings indicate that the time courses of deafening-induced striatal spine changes and acoustic changes are different. This could reflect a neural strategy of the striatum, operating upstream of the motor pathway, in shaping vocal plasticity, which need to be investigated in future.

We next examined the effect of hearing loss on ultrastructural changes in the spine synapses in adult Area X using FIB/SEM technology. We used EspINA software to identify and fully reconstruct spine synapses within a 3D volume of Area X (Fig. 3), and then directly evaluated their density and morphology. We analyzed 12 samples and 820 spine synapses, of which 6 samples and 339 synapses were obtained from 3 control birds (1–3 samples/bird), and 6 samples and 481 synapses were obtained from 3 deafened birds (2 samples/bird) 14 days after deafening. The volumes of cell somata and blood vessels, and

large myelinated axons ($> 1.5 \mu\text{m}$ in diameter or $> 5 \mu\text{m}$ in length within a section), which might have affected the estimation of the neuropil synapse density, only accounted for approximately 3% and 2% of the total volume in the 2 groups, accordingly. We observed that deafening induced a considerable increase, by approximately 61%, in the spine synapse density (Fig. 4a).

We also extracted and measured the SAS of the spine synapses to estimate their size and shape (Fig. 3b,d). By day 14 after deafening, both the SAS area (Fig. 4b, left panel) and the SAS perimeter (Fig. 4b, right panel) exhibited a slight decrease compared with those in the controls, but the differences did not reach statistical significance (area: $P = 0.14$, perimeter: $P = 0.07$; KS). We categorized the shape of spine synapses in Area X into 2 main types: macular and perforated. In the control birds, most synapses exhibited disk-shaped, macular PSDs ($73.6\% \pm 2.4\%$), with a small proportion of synapses with

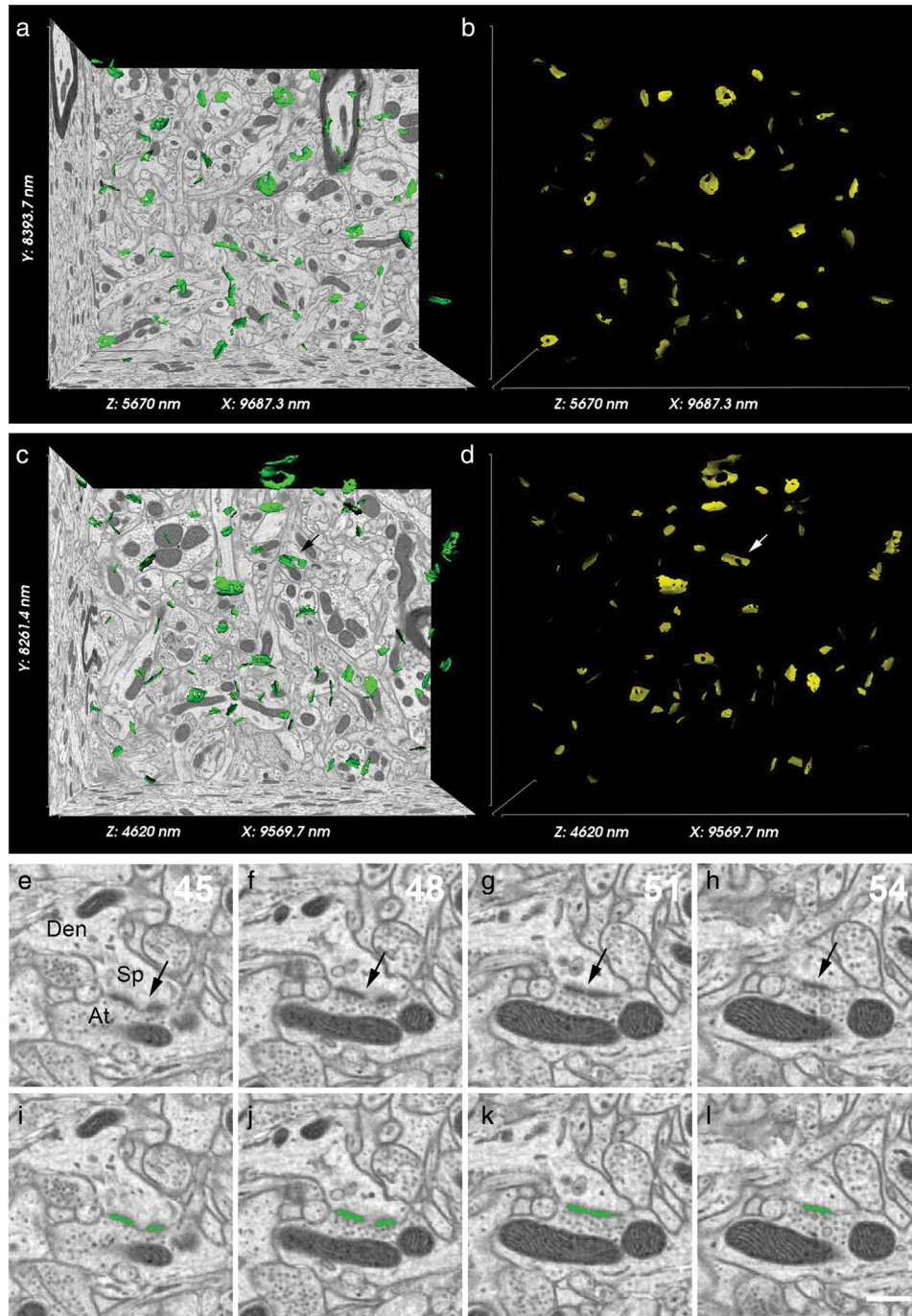


Figure 3 3D reconstructions of dendritic spine synapses in adult Area X. (a–d) Panoramic view of the reconstructed spine synapses (green) and their corresponding SAS (yellow) in a whole stack of images acquired from a control bird (a,b) or a deafened bird at 14 d after deafening (c,d) using FIB/SEM. (e–h) Sections 45, 48, 51, and 54 from the same stack of images as that shown in c and d. A synapse located on a dendritic spine (Sp) is identified in this series by a prominent PSD (arrow) and adjacent vesicles at the axon terminal (At). The spine's parent dendrite (Den) is also visible. Each section is 30-nm thick. (i–l) Segmentation of the same synapse (green) using EspINA software. The resulting 3D-reconstruction and SAS extraction are indicated with arrows in c and d, respectively. Scale bar, 500 nm.

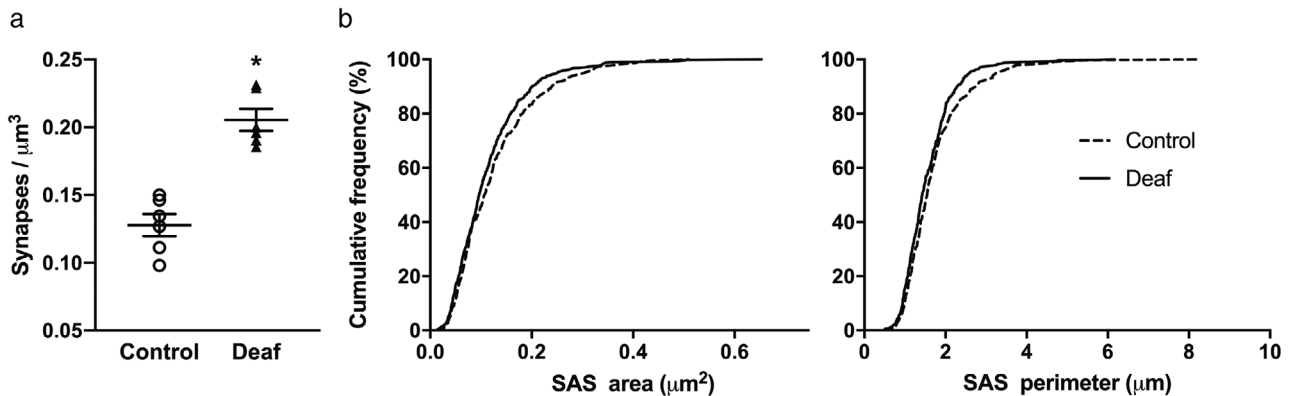


Figure 4 Effects of deafening on spine synapses in adult Area X. (a) Dot-plots of synapse density in each sample in the control and deaf conditions (with mean \pm SEM superimposed; control: 0.13 ± 0.01 synapses/ μm^3 , $n = 6$ samples; deaf: 0.21 ± 0.01 synapses/ μm^3 , $n = 6$ samples, $t_{10} = 6.721$). * $P < 0.0001$, unpaired t -test. (b) Cumulative frequency plots of the SAS area and SAS perimeter of each synapse in the 2 conditions.

perforated PSDs ($22.3\% \pm 2.5\%$). The percentages of both macular (deaf: $77.2\% \pm 2.9\%$; $t_{10} = 0.970$, $P > 0.05$, unpaired t -test) and perforated synapses (deaf: $21.5\% \pm 2.9\%$; $t_{10} = 0.206$, $P > 0.05$, unpaired t -test) in the deafened group were comparable with those in the control.

Collectively, our findings suggest that the spine length and spine synapse number in Area X are particularly sensitive to hearing loss in adult zebra finch.

DISCUSSION

We here investigated vocal-related striatal structural plasticity in response to hearing loss in adult zebra finch. Using confocal microscopy and 3D electron microscopy, we demonstrated the sensitivity of dendritic spine length and spine synapse number to auditory deprivation. Together with previous data on the effect of Area X lesions on deafening-induced vocal changes (Kojima *et al.* 2013; Zhou *et al.* 2017), we suggest that these striatal changes might contribute to adult vocal plasticity.

Dendritic spines are the key specialized structures of synaptic transmission. Considering their highly dynamic nature, they have been hypothesized to underlie the neuronal locus of structural and functional plasticity (Sala & Segal 2014; Gipson & Olive 2017). Here, we showed that the length of striatal spines within Area X rapidly increases in response to hearing loss. Longer spines are presumed to be less mature than shorter spines (Portera-Cailliau *et al.* 2003; Kim *et al.* 2008; Frotscher *et al.* 2014), and spine elongation likely reduces the strength of excitatory synapses located on spine heads (Arellano *et al.* 2007; Kim *et al.* 2008; Araya *et al.* 2014; Jasin-

ska *et al.* 2020). Hence, auditory deprivation may weaken excitatory synaptic transmission onto Area X spiny neurons, which are known to converge glutamatergic inputs from 2 pallial nuclei, the HVC (proper name) and LMAN (Farries *et al.* 2005). Dendritic spines are likely the main targets of these cortical excitatory projections, similar to their counterparts in mammals (Villalba & Smith 2018). The 2 inputs have been proposed to code distinct signals (i.e. the context and the efference copy, respectively) essential for vocal learning (Fee & Goldberg 2011; Fee 2012). Future studies should focus on distinguishing hearing-related spine changes in different pathways.

We also observed a marked increase in the number of spine synapses following hearing loss, which indicates the occurrence of excess information pathways in the local circuits upon auditory deprivation. By contrast, dendritic pruning of striatal spiny neurons with skill learning has been observed in adult rat, which likely accompanies a reduction in spine synapses and thus potentially increases signal-to-noise ratios in the striatum (Hawes *et al.* 2015). Together, we suggest that deafening-induced increases in spine length and spine synapse density lead to a reduced signal-to-noise ratio in Area X, which may serve as an important mechanism underlying song degradation, in contrast to vocal learning. These modifications of signal integration on striatal spiny neurons could, in turn, alter the activity of downstream motor pathways and result in poor performance. Indeed, we have previously reported basal ganglia-dependent spine remodeling in the adult vocal motor cortex in zebra finch after hearing loss (Zhou *et al.* 2017).

Accumulating evidence suggests that dopaminergic inputs to Area X encode reward prediction errors and shape adult vocal plasticity (Hoffmann *et al.* 2016; Hisey *et al.* 2018; Xiao *et al.* 2018; Kearney *et al.* 2019; Saravanan *et al.* 2019). Importantly, these midbrain dopaminergic neurons receive evaluative information to detect vocal error through descending auditory cortical pathways (Gale *et al.* 2008; Mandelblat-Cerf *et al.* 2014). Hence, auditory deprivation likely changes dopamine signaling within Area X. In mammals, spines are also an important target of dopaminergic inputs. These dopaminergic inputs frequently terminate onto the neck of a spine close to a glutamate axon located on the spine head, suggesting a critical role of dopamine in modulating corticostriatal synaptic transmission and plasticity (Villalba & Smith 2018). Indeed, increasing evidence indicates that dopamine strongly modulates long-term potentiation (LTP) and depression (LTD) at corticostriatal synapses on striatal spiny neurons via D1 and D2 receptors, respectively (Calabresi *et al.* 2007). Ding and Perkel (2004) confirmed a similar role of dopamine in LTP of cortical glutamatergic inputs to spiny neurons in Area X. These 2 main forms of synaptic plasticity have been shown to be associated with morphological changes in the spine (Gipson & Olive 2017). Further, dopamine modulates glutamate release from cortical inputs to striatal spiny neurons in both mammals and songbirds (Ding *et al.* 2003; Bamford *et al.* 2004), which may contribute to preventing spine loss resulting from excess excitatory drive from corticostriatal terminals (Garcia *et al.* 2010). Consequently, dopamine signaling may mediate deafening-induced spine synaptic plasticity in Area X, which should be evaluated in future studies.

In conclusion, the findings presented herein provide important structural insights into striatal plasticity in response to hearing loss, improving the understanding of the function of the basal ganglia in vocal maintenance and plasticity.

ACKNOWLEDGMENTS

This work was supported by the National Natural Science Foundation of China (31472001, 31272310). We thank the Center for Biological Imaging (CBI), Institute of Biophysics, Chinese Academy of Science, for our electron microscopy and we are grateful to Li Wang and Jianguo Zhang for their help in making EM samples and taking EM images. We thank Félix for his step-by-step instructions to use EspINA. We thank Jin Liu for his help in confocal imaging.

REFERENCES

- Araya R, Vogels TP, Yuste R (2014). Activity-dependent dendritic spine neck changes are correlated with synaptic strength. *PNAS* **111**, E2895–904.
- Arellano JI, Benavides-Piccione R, Defelipe J, Yuste R (2007). Ultrastructure of dendritic spines: Correlation between synaptic and spine morphologies. *Frontiers in Neuroscience* **1**, 131–43.
- Bamford NS, Robinson S, Palmiter RD, Joyce JA, Moore C, Meshul CK (2004). Dopamine modulates release from corticostriatal terminals. *Journal of Neuroscience* **24**, 9541–52.
- Brainard MS, Doupe AJ (2000). Interruption of a basal ganglia-forebrain circuit prevents plasticity of learned vocalizations. *Nature* **404**, 762–6.
- Bolhuis JJ, Okanoya K, Scharff C (2010). Twitter evolution: Converging mechanisms in birdsong and human speech. *Nature Reviews Neuroscience* **11**, 747–59.
- Calabresi P, Picconi B, Tozzi A, Di Filippo M (2007). Dopamine-mediated regulation of corticostriatal synaptic plasticity. *Trends in Neuroscience (Tins)* **30**, 211–9.
- Chen CC, Lu J, Zuo Y (2014). Spatiotemporal dynamics of dendritic spines in the living brain. *Frontiers in Neuroanatomy* **8**, 28.
- Chidambaram SB, Rathipriya AG, Bolla SR *et al.* (2019). Dendritic spines: Revisiting the physiological role. *Progress in Neuro-Psychopharmacology & Biological Psychiatry* **92**, 161–93.
- Ding L, Perkel DJ (2002). Dopamine modulates excitability of spiny neurons in the avian basal ganglia. *Journal of Neuroscience* **22**, 5210–8.
- Ding L, Perkel DJ (2004). Long-term potentiation in an avian basal ganglia nucleus essential for vocal learning. *Journal of Neuroscience* **24**, 488–94.
- Ding L, Perkel DJ, Farries MA (2003). Presynaptic depression of glutamatergic synaptic transmission by D1-like dopamine receptor activation in the avian basal ganglia. *Journal of Neuroscience* **23**, 6086–95.
- Doupe AJ, Perkel DJ, Reiner A, Stern EA (2005). Bird-brains could teach basal ganglia research a new song. *Trends in Neuroscience (Tins)* **28**, 353–63.
- Farries MA, Ding L, Perkel DJ (2005). Evidence for “direct” and “indirect” pathways through the song system basal ganglia. *Journal of Comparative Neurology* **484**, 93–104.
- Farries MA, Perkel DJ (2002). A telencephalic nucleus essential for song learning contains neurons with

- physiological characteristics of both striatum and globus pallidus. *Journal of Neuroscience* **22**, 3776–87.
- Fazl A, Fleisher J (2018). Anatomy, physiology, and clinical syndromes of the basal ganglia: a brief review. *Seminars in Pediatric Neurology* **25**, 2–9.
- Fee MS, Goldberg JH (2011). A hypothesis for basal ganglia-dependent reinforcement learning in the songbird. *Neuroscience* **198**, 152–70.
- Fee MS (2012). Oculomotor learning revisited: A model of reinforcement learning in the basal ganglia incorporating an efference copy of motor actions. *Frontiers in Neural Circuits* **6**, 38.
- Frotscher M, Studer D, Graber W, Chai X, Nestel S, Zhao S (2014). Fine structure of synapses on dendritic spines. *Frontiers in Neuroanatomy* **8**, 94.
- Gale SD, Perkel DJ (2010). Anatomy of a songbird basal ganglia circuit essential for vocal learning and plasticity. *Journal of Chemical Neuroanatomy* **39**, 124–31.
- Gale SD, Person AL, Perkel DJ (2008). A novel basal ganglia pathway forms a loop linking a vocal learning circuit with its dopaminergic input. *Journal of Comparative Neurology* **508**, 824–39.
- Garcia BG, Neely MD, Deutch AY (2010). Cortical regulation of striatal medium spiny neuron dendritic remodeling in parkinsonism: modulation of glutamate release reverses dopamine depletion-induced dendritic spine loss. *Cerebral Cortex* **20**, 2423–32.
- Gipson CD, Olive MF (2017). Structural and functional plasticity of dendritic spines - root or result of behavior? *Genes, Brain, and Behavior* **16**, 101–17.
- Goldberg JH, Adler A, Bergman H, Fee MS (2010). Singing-related neural activity distinguishes two putative pallidal cell types in the songbird basal ganglia: Comparison to the primate internal and external pallidal segments. *Journal of Neuroscience* **30**, 7088–98.
- Goldberg JH, Fee MS (2010). Singing-related neural activity distinguishes four classes of putative striatal neurons in the songbird basal ganglia. *Journal of Neurophysiology* **103**, 2002–14.
- Graybiel AM (2005). The basal ganglia: Learning new tricks and loving it. *Current Opinion in Neurobiology* **15**, 638–44.
- Graybiel AM, Aosaki T, Flaherty AW, Kimura M (1994). The basal ganglia and adaptive motor control. *Science* **265**, 1826–31.
- Hawes SL, Evans RC, Unruh BA *et al.* (2015). Multimodal plasticity in dorsal striatum while learning a lateralized navigation task. *Journal of Neuroscience* **35**, 10535–49.
- Hisey E, Kearney MG, Mooney R (2018). A common neural circuit mechanism for internally guided and externally reinforced forms of motor learning. *Nature Neuroscience* **21**, 589–97.
- Hoffmann LA, Saravanan V, Wood AN, He L, Sober SJ (2016). Dopaminergic contributions to vocal learning. *Journal of Neuroscience* **36**, 2176–89.
- Horita H, Wada K, Jarvis ED (2008). Early onset of deafening-induced song deterioration and differential requirements of the pallial-basal ganglia vocal pathway. *European Journal of Neuroscience* **28**, 2519–32.
- Horita H, Kobayashi M, Liu WC, Oka K, Jarvis ED, Wada K (2012). Specialized motor-driven *dusp1* expression in the song systems of multiple lineages of vocal learning birds. *PLoS ONE* **7**, e42173.
- Ingham CA, Hood SH, Arbuthnott GW (1989). Spine density on neostriatal neurones changes with 6-hydroxydopamine lesions and with age. *Brain Research* **503**, 334–8.
- Jarvis ED (2019). Evolution of vocal learning and spoken language. *Science* **366**, 50–4.
- Jasinska M, Woznicka O, Jasek-Gajda E, Lis GJ, Pyza E, Litwin JA (2020). Circadian changes of dendritic spine geometry in mouse barrel cortex. *Frontiers in Neuroscience* **14**, 578881.
- Kearney MG, Warren TL, Hisey E, Qi J, Mooney R (2019). Discrete evaluative and premotor circuits enable vocal learning in songbirds. *Neuron* **104**, 559–75.e6.
- Kim BG, Dai HN, McAtee M, Bregman BS (2008). Modulation of dendritic spine remodeling in the motor cortex following spinal cord injury: Effects of environmental enrichment and combinatorial treatment with transplants and neurotrophin-3. *Journal of Comparative Neurology* **508**, 473–86.
- Kojima S, Kao MH, Doupe AJ (2013). Task-related “cortical” bursting depends critically on basal ganglia input and is linked to vocal plasticity. *PNAS* **110**, 4756–61.
- Kreitzer AC, Malenka RC (2008). Striatal plasticity and basal ganglia circuit function. *Neuron* **60**, 543–54.
- Li J, Zhou X, Huang L *et al.* (2013). Alteration of CaBP expression pattern in the nucleus magnocellularis following unilateral cochlear ablation in adult zebra finches. *PLoS ONE* **8**, e79297.
- Lombardino AJ, Nottebohm F (2000). Age at deafening affects the stability of learned song in adult male zebra finches. *Journal of Neuroscience* **20**, 5054–64.

- Mandelblat-Cerf Y, Las L, Denisenko N, Fee MS (2014). A role for descending auditory cortical projections in songbird vocal learning. *elife* **3**, e02152, <https://doi.org/10.7554/eLife.02152>
- McNeill TH, Brown SA, Rafols JA, Shoulson I (1988). Atrophy of medium spiny I striatal dendrites in advanced Parkinson's disease. *Brain Research* **455**, 148–52.
- Merchán-Pérez A, Rodríguez JR, Alonso-Nanclares L, Schertel A, Defelipe J (2009). Counting synapses using FIB/SEM microscopy: A true revolution for ultrastructural volume reconstruction. *Frontiers in Neuroanatomy* **3**, 18.
- Morales J, Alonso-Nanclares L, Rodríguez JR, DeFelipe J, Rodríguez Á, Merchán-Pérez Á (2011). Espina: a tool for the automated segmentation and counting of synapses in large stacks of electron microscopy images. *Frontiers in Neuroanatomy* **5**, 18.
- Morales J, Rodríguez A, Rodríguez JR, DeFelipe J, Merchán-Pérez A (2013). Characterization and extraction of the synaptic apposition surface for synaptic geometry analysis. *Frontiers in Neuroanatomy* **7**, 20.
- Nordeen KW, Nordeen EJ (1992). Auditory feedback is necessary for the maintenance of stereotyped song in adult zebra finches. *Behavioral & Neural Biology* **57**, 58–66.
- Perrin E, Venance L (2019). Bridging the gap between striatal plasticity and learning. *Current Opinion in Neurobiology* **54**, 104–12.
- Pfenning AR, Hara E, Whitney O *et al.* (2014). Convergent transcriptional specializations in the brains of humans and song-learning birds. *Science* **346**, 1256846.
- Portera-Cailliau C, Pan DT, Yuste R (2003). Activity-regulated dynamic behavior of early dendritic protrusions: Evidence for different types of dendritic filopodia. *Journal of Neuroscience* **23**, 7129–42.
- Raghanti MA, Edler MK, Stephenson AR *et al.* (2016). Human-specific increase of dopaminergic innervation in a striatal region associated with speech and language: A comparative analysis of the primate basal ganglia. *Journal of Comparative Neurology* **524**, 2117–29.
- Rodríguez A, Ehlenberger DB, Dickstein DL, Hof PR, Wearne SL (2008). Automated three-dimensional detection and shape classification of dendritic spines from fluorescence microscopy images. *PLoS ONE* **3**, e1997.
- Sala C, Segal M (2014). Dendritic spines: The locus of structural and functional plasticity. *Physiological Reviews* **94**, 141–88.
- Saravanan V, Hoffmann LA, Jacob AL, Berman GJ, Sober SJ (2019). Dopamine depletion affects vocal acoustics and disrupts sensorimotor adaptation in songbirds. *eNeuro* **6**, e0190-19.2019.
- Simmonds AJ, Leech R, Iverson P, Wise RJ (2014). The response of the anterior striatum during adult human vocal learning. *Journal of Neurophysiology* **112**, 792–801.
- Simonyan K, Horwitz B, Jarvis ED (2012). Dopamine regulation of human speech and bird song: a critical review. *Brain and Language* **122**, 142–50.
- Tchernichovski O, Nottebohm F, Ho CE, Pesaran B, Mitra PP (2000). A procedure for an automated measurement of song similarity. *Animal Behaviour* **59**, 1167–76.
- Thompson JA, Perkel DJ (2011). Endocannabinoids mediate synaptic plasticity at glutamatergic synapses on spiny neurons within a basal ganglia nucleus necessary for song learning. *Journal of Neurophysiology* **105**, 1159–69.
- Tschida KA, Mooney R (2012). Deafening drives cell-type-specific changes to dendritic spines in a sensorimotor nucleus important to learned vocalizations. *Neuron* **73**, 1028–39.
- Villalba RM, Mathai A, Smith Y (2015). Morphological changes of glutamatergic synapses in animal models of Parkinson's disease. *Frontiers in Neuroanatomy* **9**, 117.
- Villalba RM, Smith Y (2018). Loss and remodeling of striatal dendritic spines in Parkinson's disease: From homeostasis to maladaptive plasticity? *Journal of Neural Transmission* **125**, 431–47.
- Xiao L, Chattree G, Oscos FG, Cao M, Wanat MJ, Roberts TF (2018). A basal ganglia circuit sufficient to guide birdsong learning. *Neuron* **98**, 208–21.
- Xiong Q, Znamenskiy P, Zador AM (2015). Selective corticostriatal plasticity during acquisition of an auditory discrimination task. *Nature* **521**, 348–51.
- Zhou X, Fu X, Lin C *et al.* (2017). Remodeling of dendritic spines in the avian vocal motor cortex following deafening depends on the basal ganglia circuit. *Cerebral Cortex* **27**, 2820–30.

SUPPLEMENTARY MATERIALS

Additional supporting information may be found online in the Supporting Information section at the end of the article.

Figure S1 Scatter plots of the distributions of changes in the mean entropy (A) and entropy variance (B) of each syllable in the 3 groups in the same dataset as in Fig. 2 (one point per syllable; control: 38 syllables from 9 birds, deaf 3d: 31 syllables from 8 birds, deaf 14d: 29 syllables from 8 birds). The horizontal line within each plot denotes the median. Changes to syllables are presented as percentage of baseline, determined as described in Methods.

Cite this article as:

Zhou X, Chen Y, Peng J, Zuo M, Sun Y (2021). Deafening-induced rapid changes to spine synaptic connectivity in the adult avian vocal basal ganglia. *Integrative Zoology* **00**, 1–11.